Int j simul model 24 (2025) 3, 521-532
Original scientific paper

RESEARCH ON LIGHTWEIGHTING OF KEY COMPONENTS OF LIGHT VEHICLE DRIVE SHAFTS

Zhao, C. L.*; Guo, L. H.**,#; Liang, H. M.**; Xi, L.*; Tang, H.** & Wu, D.*
* Geely University of China, Chengdu 641423, China
** Chengdu Jincheng College, Chengdu 611731, China
E-Mail: guo_lihong123@126.com (# Corresponding author)

Abstract
As a critical component of the vehicle power transmission system, the structural design and performance analysis of the drive shaft significantly influence the fuel economy, performance, and safety of the vehicle. This study focuses on the lightweight design of the drive shaft for light vehicles. By modelling the geometric parameters of the drive shaft, defining material properties, and utilizing Finite Element Analysis (FEA) software, the relevant performances such as stress, strain, and displacement of the component structure were comprehensively analysed. Based on the stress distribution results, an optimized design of the drive shaft structure was conducted to enhance its load-bearing capacity and service life. Through this optimization process, the lightweighting of the drive shaft for light vehicles was achieved while ensuring sufficient strength. The mass of the flange fork and universal joint fork components of the drive shaft was reduced by 4.31 % and 11.47 %, respectively, thereby improving the fuel economy and overall performance of the vehicle.
(Received in June 2025, accepted in July 2025. This paper was with the authors 1 month for 1 revision.)

Key Words: Automobile Drive Shaft, Lightweighting, ANSYS, Static Force Analysis

1. INTRODUCTION

With the development of the automotive industry, improving energy utilization efficiency and reducing carbon dioxide emissions have become key issues that need to be considered in energy development [1]. Faced with the continuous need for in-depth research on cost and energy issues, lightweight treatment of automobiles can reduce fuel consumption, and lightweight technology has become the key for various automotive enterprises to enhance their market competitiveness [2]. Lightweight technology aims to ensure the performance and safety standards of automobiles while reducing the curb weight of vehicles through the application of new materials, improved processes, and enhanced designs, thereby improving fuel efficiency, reducing emissions, enhancing performance, and improving handling [3, 4].

The drive shaft is an important component in the automotive power transmission system. Its structural design and performance research are of great significance to the overall performance and reliability of the vehicle [5]. The lightweighting of the drive shaft is a key demand and implementation approach for the lightweighting of light vehicles. It can reduce the weight and moment of inertia of the transmission system and improve dynamic response and transmission efficiency. Traditional research focuses more on lightweight research from the material direction or structural optimization through single software simulation. In this study, structural lightweighting was carried out through the Altair series software, and the lightweighting results were verified in combination with Ansys, thereby achieving cross-platform simulation structure optimization. Compared with the traditional structural lightweighting simulation methods, the results are more reliable. The main contributions are as follows: (1) A static analysis and lightweight design idea for the transmission shaft component of light vehicles was proposed. Through static analysis, a scientific basis was provided for lightweight design. Then, the structure of the transmission shaft component was optimized and verified to achieve the lightweight goal. (2) By analysing and evaluating the strength and stiffness of the transmission shaft, the stress and deformation were analysed, and the design was optimized to enhance performance. By integrating lightweight research, we aim to reduce costs, enhance transmission efficiency and reliability, and promote technological innovation and sustainable development. (3) Through structural optimization design, the load-bearing capacity, rigidity and durability of the drive shaft have been enhanced, thereby improving the vehicle's acceleration, handling and reliability.

2. RELATED WORKS

Currently, research on the lightweight design of automotive drive shafts primarily centres on enhancing various aspects such as materials, structural configurations, fatigue resistance, and multi-physical field coupling, aiming to achieve weight reduction while maintaining or improving performance and reliability. Presently, two major directions dominate this field: material enhancement and structural optimization. For example, the selection of materials and manufacturing techniques significantly influences the mechanical properties and service life of drive shafts. Reddy and Nagaraju [6] performed a finite element comparative analysis between composite and steel shafts using lightweight composite materials, demonstrating that vehicle weight can be effectively reduced without compromising quality or reliability. The study ensured torsional frequency, buckling resistance, and natural bending characteristics were maintained while achieving weight savings. Zhang et al. [7] proposed a multi-scale reliability-based optimization design method for carbon fibre reinforced plastic (CFRP) drive shafts. By parametrically modelling microscale components and employing two homogenization approaches to estimate elastic properties, the influence of micro-level parameter variations on composite performance was investigated. Their findings revealed that CFRP drive shafts designed through this approach achieved a weight reduction of over 30 % compared to traditional metallic counterparts. Samuel and Tayong [8] conducted simulation analyses on multi-layered material drive shafts using COMSOL Multiphysics software. Results indicated that CFRP shafts exhibited the highest fundamental natural frequency and could endure applied loads within the expected fatigue life. These shafts also demonstrated the highest fatigue service coefficient and critical buckling torque, with a weight reduction of 40.7 % compared to aluminium tubes and 79.6 % compared to steel tubes.

Choi et al. [9] and Tian et al. [10] optimized the geometric configuration, connection methodology, and wall thickness distribution of components under actual operating conditions by integrating finite element analysis with experimental validation. Research by Harl et al. demonstrated that this approach can significantly reduce component weight [11]. Kim et al. [12] performed shape optimization of a drive shaft using Design of Experiments (DOE) and the Kriging model. Nine shape design parameters were selected through case studies, taking into account the geometrical characteristics of the components. The results of the shape optimization revealed that the maximum torsional stress in the optimized drive shaft was reduced by 11.5 %, its fatigue life increased by 3.7 times, and its weight decreased by approximately 25 %. In addition, Donmez and Kahraman [13], Chen et al. [14] and others analysed the influence of multi-physics coupling effects on the performance of transmission shafts, considering that such shafts may be subjected to combined loads – including mechanical forces, thermal effects, and vibrations – during actual operation [15, 16]. Multi-physics coupling is typically achieved by analysing coupled deformations under various operating conditions, such as variations in friction coefficient and bending roller force [17]. This coupling approach can also be effectively applied to fault analysis and diagnosis [18]. Teli et al. [19] successfully addressed the issue of oil seal leakage in a transmission system by implementing the structured DMADV (Define, Measure, Analyse, Design, and Verify) methodology.

3. RESEARCH METHOD

3.1 Basic composition of drive shafts and lightweight thinking

In the automotive powertrain system, the drive shaft serves as a critical component for transmitting engine power to the wheels. In front-engine rear-wheel drive configurations, it connects the transmission to the main reducer, while in four-wheel drive systems, it distributes power via the transfer case. The drive shaft must possess high strength, rigidity, and durability to ensure reliable performance. Cross-axis universal joint drive shafts are extensively utilized in commercial vehicles and front-wheel/four-wheel drive passenger cars due to their ease of manufacturing and capability to handle high torque. These drive shafts consist of a shaft tube and universal joint assemblies. The lightweight design process involves the following steps:

(1) Defining performance targets and selecting appropriate materials;
(2) Establishing a CAD model for load analysis;
(3) Conducting finite element analysis to obtain stress, strain, and fatigue life parameters;
(4) Optimizing the structural design, validating performance, and ultimately formulating an improvement plan.

Figure 1: Schematic diagram of a typical drive shaft.

3.2 Lightweight methods

Automotive lightweighting can be achieved through structural optimization, the use of lightweight materials, and advanced manufacturing technologies. Structural optimization reduces costs by enhancing design efficiency. The application of lightweight materials in commercial vehicles is currently restricted due to process limitations and high costs. This study focuses on the flange fork and splined shaft fork of the drive shaft assembly. Based on OptiStruct topology optimization, the SIMP variable density method is employed for optimization, with rigidity strength serving as the constraint and volume minimization as the objective. Although carbon fibre has not yet been widely commercialized due to cost and process challenges, advancements in finite element analysis and computing hardware have enabled topology optimization to be extensively applied to components such as frames and transmission systems, ensuring optimal performance at minimal weight. The three key elements of structural optimization include design variables (adjustable parameters), constraint conditions (technological limitations), and objective functions (optimization goals), which collectively ensure that the design satisfies technical requirements. The optimized mathematical model can be described as follows:

Minimize: $$f(x) = f(x_1, x_2, \dots, x_n) \tag{1}$$

Subject to: $$f(x) = g_j(x) \le 0, \;\; j = 1, \dots, m_j \tag{2}$$

$$h_k(x) \le 0, \;\; k = 1, \dots, m_k \tag{3}$$

In topology optimization, the design variable $x = (x_1, ..., x_n)$ regulates the key parameters of the structure. The objective function $f(x)$ drives performance optimization (e.g., strain energy, volume), while the constraint conditions g(x) and h(x) define boundaries for displacement, stress, etc. This method enhances efficiency by optimizing material distribution and encompasses three primary approaches: the variable thickness method optimizes thin-walled structures via unit thicknesses (with limitations in three-dimensional applications); the homogenization method employs proportional distributions of microporous materials, requiring post-processing to simplify configurations; and the variable density method defines elastic modulus based on unit density, distinguishes material regions through 0-1 density values, and improves manufacturability by incorporating penalty factors and SIMP/RAMP interpolations. The optimization model consists of three fundamental components: design variables, objective functions, and constraint conditions. While this approach improves material utilization, future developments will focus on algorithmic innovation, practicality enhancement, and the expansion of multi-field applications.

4. THE SIMULATION EXPERIMENT

4.1 Experimental platform

In this experiment, the Altair HyperMesh setting was used to perform mesh division and topology optimization parameter setting for the key parts of the drive shaft, namely the flange fork and the universal joint fork, and the topology optimization was carried out using Altair OptiStruct. The Altair series of software is widely used in aerospace, automotive and other fields for structural analysis and optimization. Combined with advanced algorithms, it helps reduce weight, improve performance and optimize material usage. Meanwhile, to verify the optimization effect, Ansys Workbench was used to conduct a comparative analysis of the mechanical properties of the models before and after optimization.

4.2 Lightweighting process of drive shafts

• **Establish the drive shaft model:** This study conducts a development and analysis of the drive shaft assembly of a certain enterprise. Based on the design data, a SOLIDWORKS 3D model was established and converted into *stp* format to be imported into Altair HyperMesh to complete meshing and finite element analysis, laying the foundation for structural optimization.

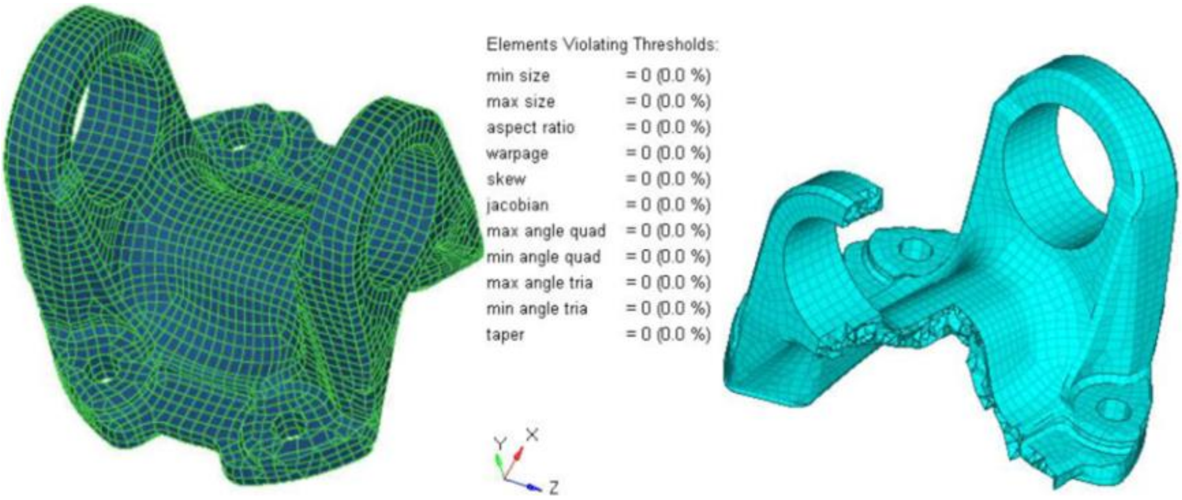

Figure 2: Qualified 2D meshes and 3D meshes.

• **Mesh partitioning:** In Altair HyperMesh, two-dimensional mesh partitioning is implemented first. A 5 mm size is set and a quadrilateral/triangular hybrid mesh is adopted to adapt the surface. The mesh is automatically allocated according to the part parameters through the *automesh* function.

• **Mesh optimization:** Use quality index to detect the quality of two-dimensional meshes, automatically repair defective meshes through *elem cleanup*, and manually correct residual problems. Finally, a three-dimensional model was generated using tetrahedral meshes, taking into account both geometric accuracy and computational efficiency. The effect is shown in Fig. 2.

• **Parameter settings:** After the model meshing is completed and exported as a *cdb* format file, the next step is to import it into the Workbench module of Ansys software for subsequent processing. Immediately after that, material properties such as elastic modulus and Poisson's ratio parameters need to be defined in the Engineering Data module. These key physical properties are crucial for ensuring the authenticity and reliability of the analysis results. The relevant parameters are shown in Table I.

Table I: Material properties.

Part	**Name of the material**	**Elasticity modulus** /GPa	**Poisson's ratio**	**Yield strength** /MPa	**Density** /g/cm^3
Flange Yoke	40Cr	211	0.28	785	7.87
Universal Joint Fork	40Cr	211	0.28	785	7.87

• **Workbench conducts performance analysis of key parts of the drive shaft:** Static torsional strength and stiffness are the core performance indicators of the automotive drive shaft assembly. The analysis results are used to evaluate design compliance, provide benchmark data for bench tests to compare with actual results, and serve as important constraints for topology optimization. Fatigue failure, without obvious warning signs, becomes the main failure mode of drive shafts. Therefore, torsional fatigue life analysis is the core basis for determining product compliance and safety, which can predict the long-term reliability of test pieces and ensure performance and service life under various working conditions.

(1) Finite element analysis of flange forks

The flange fork, as the core component of the drive shaft system, is responsible for transmitting the engine power to the main reducer through the cross shaft. In the component analysis, a torque of 10000 N·m equivalent to the rated torque of the drive shaft needs to be applied to its ear hole, and a fixed support constraint is set at the end face to simulate the actual assembly state. This boundary condition setting enables the finite element analysis to accurately reflect the force-induced deformation characteristics of the flange fork. The relevant simulation results are detailed in Fig. 3. In Fig. 3 a is the boundary condition diagram; in Fig. 3 b is the stress cloud map; in Fig. 3 c is the cloud map of the x-direction displacement; in Fig. 3 d is the fatigue life cloud map.

The results show that the maximum stress of 437.08 MPa is lower than the yield strength of 785 MPa, and the safety factor of 1.8 meets the standard. The maximum deformation is 0.32345 mm and the stiffness value is 1.66 °/m, which is superior to the industry standard. The fatigue life reaches 297,070 cycles, exceeding the standard by 150,000 times. Analysis shows that the material utilization rate in the turtle back area and near the mounting plate is low, and the lifespan of most areas far exceeds the requirements, leaving room for lightweighting. Optimizing structural materials can reduce weight while maintaining performance. It is necessary to focus on monitoring the stress concentration area. The safety margin in the remaining areas is sufficient and has the potential for further optimization.

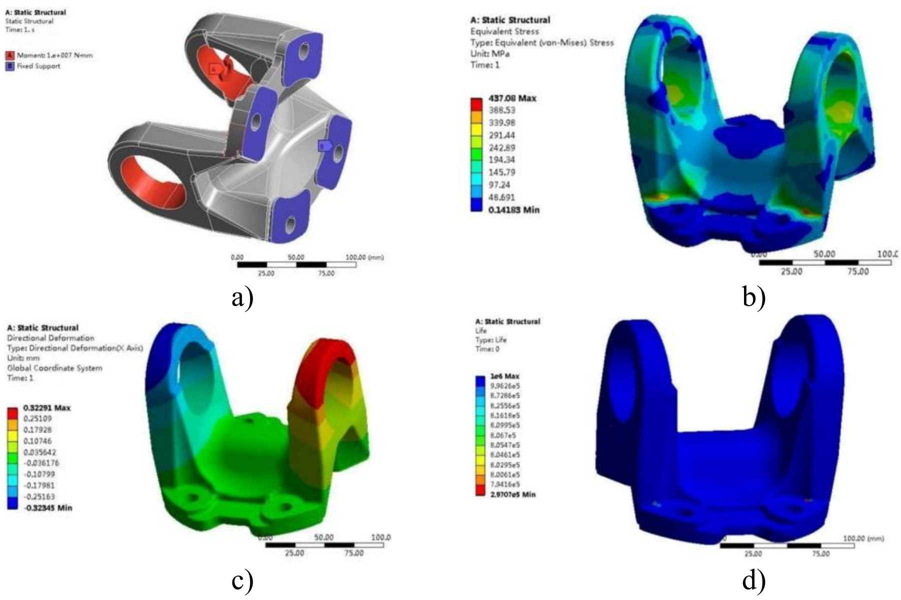

Figure 3: Finite element analysis results.

(2) Finite element analysis of universal joint fork

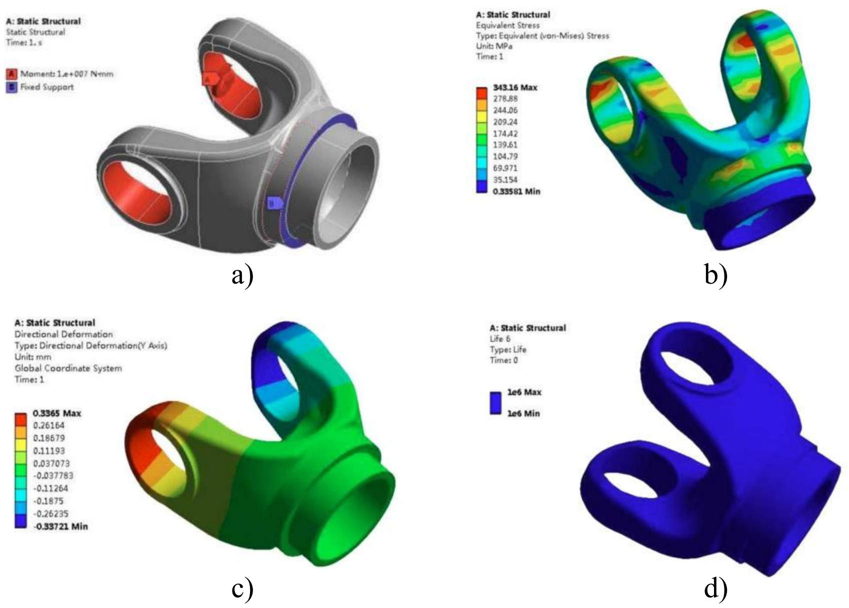

Figure 4: Finite element analysis results.

When studying the mechanical behaviour of the universal joint fork, attention should be paid to the path by which the torque is transmitted through the ear hole via the cross shaft to the fork body. When modelling, the welding area between the fork and the shaft tube is set as a rigid connection without displacement or deformation, and the connection end is regarded as a fixed support. The analysis boundary conditions are set as follows: a torque of 10,000 N·m is applied to the fork ear hole, and the welding end face is fixed and constrained to simulate the actual working conditions and accurately evaluate the structural performance. The relevant simulation results are detailed in Fig. 4. In Fig. 4 a is the boundary condition diagram; in Fig. 4 b is the stress cloud map; Fig. 4 c represents the Y-direction displacement cloud map; in Fig. 4 d is the fatigue life cloud map.

The analysis results show that the maximum stress is 343.16 MPa and the safety factor is 2.29, which meets the minimum requirement of 1.50. The torsional stiffness of 1.51 °/m meets the design requirement of 15 °/m. Technical requirements for fatigue life exceeding 150,000 times after 1 million times. The stress displacement in the fork area is relatively low, and its contribution to the overall strength is limited. Life analysis indicates that its durability is significantly higher than the requirements of the drive shaft, confirming that the universal joint fork has the space for lightweight under the premise of meeting the performance.

• **Topology Structure Optimization:** After setting the working conditions through Altair Hyper Mesh, the topology optimization parameters need to be configured. The relative density of the design area units is defined as a variable based on the variable density method, and the topological parameters are set using the preset Property attribute. The Altair OptiStruct optimization is then utilized to introduce manufacturability constraints, such as the minimum member size, to ensure uniform size and processing stiffness that meets the requirements (Fig. 5).

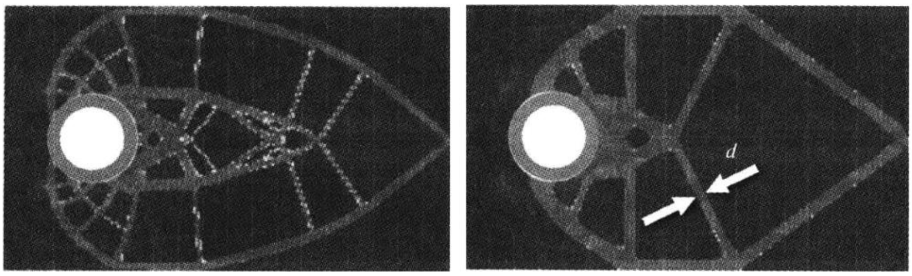

Figure 5: Effect of minimum member size constraints.

Topology optimization requires setting the minimum member size to ensure manufacturability and avoid overly fine structures. HyperMesh configures this parameter through *mindim* in the Parameters menu of the Topology panel. In engineering practice, it is usually taken as three times the average size of the unit.

(1) Setting of flange fork optimization parameters

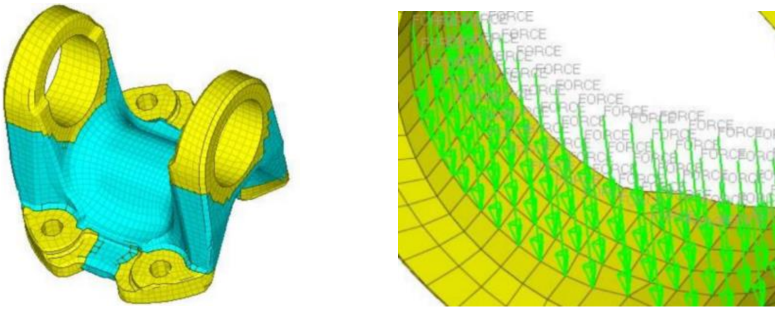

a) b)

Figure 6: Setting of the optimization parameters for the flange fork.

The flange fork mesh model was constructed in the front, including two universal joint ear holes and four bolt hole mounting discs. The ear holes and mounting discs are set as fixed non-design areas, while the rest are optimizable areas. Create a new Component using HyperMesh to store non-design units (distinguishable by yellow and blue, as shown in Fig. 6 a, the design area and non-design area of the flange cross), define homogeneous materials with an elastic modulus of 211 GPa and a Poisson's ratio of 0.28, and ensure that the materials in the design domain and the non-design domain are the same. During the analysis, the end face of the flange fork was fixed, and a reverse distributed load was applied to the ear hole to simulate the torque of the cross axis. See Fig. 6 b, for a local enlarged view of the boundary conditions of the flange fork.

(2) Setting of universal joint fork optimization parameters

The finite element model of the universal joint fork was optimized by the variable density method, and the element density in the design area was set as a topological variable. In the Analysis module, configure the optimization parameters, create two attribute units and define the unit density. Adding a minimum size constraint of 20 mm and a plane scale limits the maximum stress of the element to 343 MPa and the Y-direction displacement of the node to ±0.336/0.337 mm to achieve weight reduction. The final set stress is 344 MPa and the displacement is ±0.34 mm to ensure that the static stiffness and static strength meet the standards. When optimizing the topology, the ear hole and the step axis are set as the non-design area (yellow), and the rest are the adjustable design area (blue). The HyperMesh partitioning is shown in Fig. 7 a for the universal joint fork design area and the non-design area. The material parameters follow the configuration of the flange fork. The boundary conditions include applying torque to the ear hole and fixing the large end face of the stepped shaft. The torque of the cross shaft is equivalent to the uniform distribution of the load on the two half cylindrical surfaces. The response under the model working conditions was verified through load step static analysis, as shown in Fig. 7 b, a local magnification of the universal joint fork boundary condition.

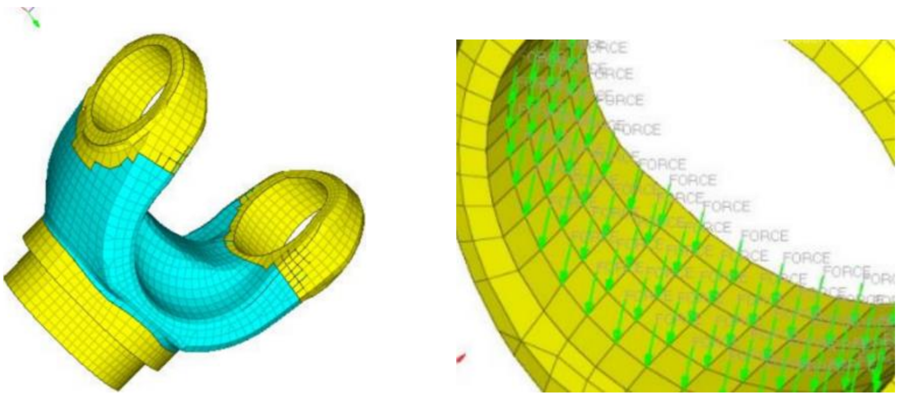

a) b)

Figure 7: Setting of the optimization parameters for universal joint forks.

• **Workbench conducts optimized structure verification:** The optimized structure is imported into the Workbench module of Ansys software with the same parameter Settings for component performance analysis to verify the lightweight design effect.

4.3 Topological optimization results of key parts

• **Optimization results of flange fork topology**

After defining the flange fork attributes and boundaries, topology optimization was carried out using OptiStruct, which was completed after 13 iterations. Each iteration adjusts the material distribution to minimize the volume and meet the requirements of strength displacement. The volume decreases rapidly in the early stage and fluctuates in the later stage, reflecting a dynamic balance. OptiStruct sets a minimum cell density of 0.01 to prevent premature cell deletion. Fig. 8 a shows the optimization model: The red unit (density ≈ 1) is the critical area, and the dark blue (≈ 0.01) is the unnecessary area. The distribution is consistent with the previous low-stress area, verifying its effectiveness. Optimization requires the elimination of low-contribution units. The density threshold balances practicality and processability. In this example, the minimum threshold of 0.15 is retained. If it is lower than, it will be eliminated to ensure lightweight and meet the process requirements of strength and stiffness. The result is shown in Fig. 8 b. The unit between the central turtle back and the mounting plate has been removed.

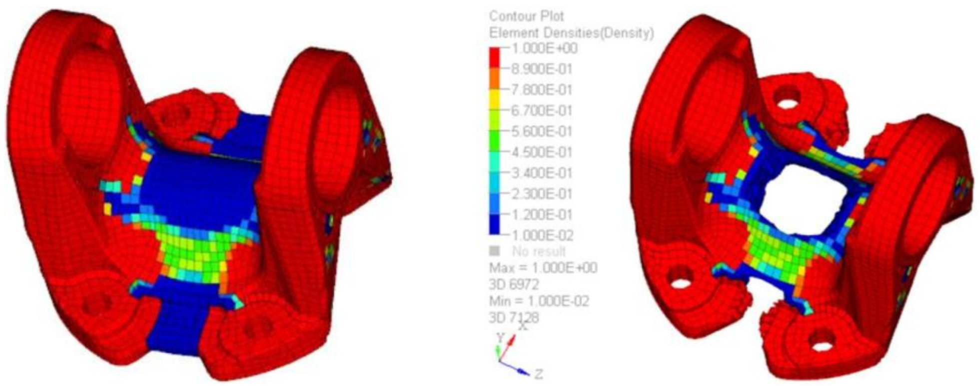

a) b)

Figure 8: Optimization results of the flange fork topology.

- **Optimization results of universal joint fork topology**

The universal joint fork has been iteratively eliminated from the inefficient structural areas, and its curve is smoother than that of the flange fork, which is due to the difference between the structural characteristics and the initial material. In the subsequent iterations, the objective function fluctuates and decreases due to the fine-tuning of variables by the algorithm. The universal joint fork and the splined axis fork show converging fluctuations due to structural similarity. Fig. 9 a shows the optimization results: The red high-density area (nearly 1) is the key load-bearing area, and the blue low-density area bears less stress. The density elements (close to 0.01) are distributed in the low-stress area, and their removability is verified by static analysis. Lightweighting requires the removal of low-contribution elements. Assuming the minimum element density is 0.3, the excess elements are removed to form a new topology (Figs. 9 b and 9 c). A large number of elements inside the universal joint fork and on both sides of the fork are removed.

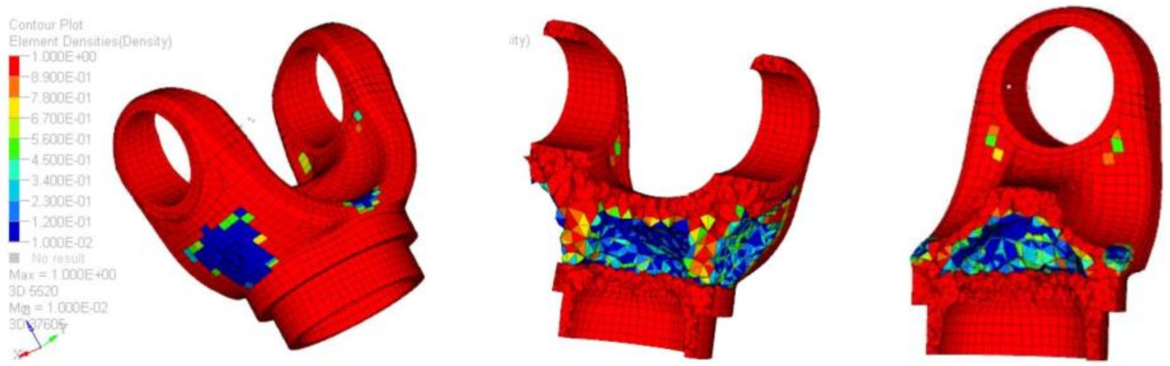

a) b) c)

Figure 9: Optimization results of the universal joint fork topology.

4.4 Optimization results and analysis

Based on the topology optimization results of the flange fork in Fig. 8, a finite element analysis was conducted on the improved model. Use the same methods and techniques as before to set the parameters for grid division. Material properties were added, and the working condition boundary conditions were set. Solution result: The stress cloud map (Fig. 10 a) presents the stress distribution. The displacement cloud map (Fig. 10 b) shows the displacement conditions. Fatigue life cloud map (Fig. 10 c) reveals the life distribution to assess durability and predict fatigue failure.

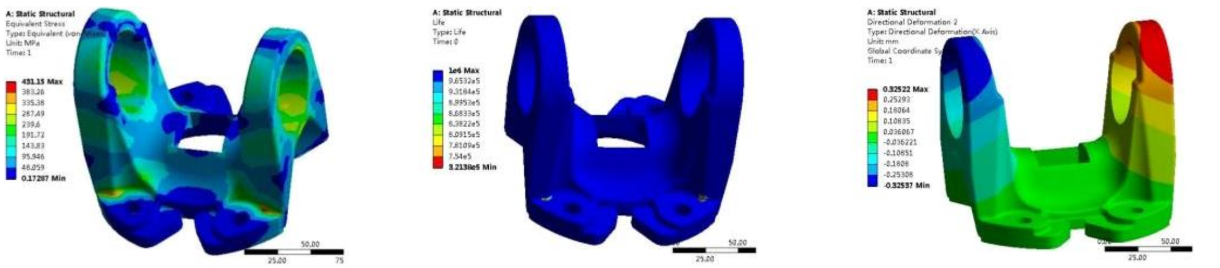

a) b) c)

Figure 10: Finite element analysis results of the improved flange fork model.

Fig. 10 shows that the improved model performance of the flange fork is as follows: The maximum stress is 431 MPa (lower than the yield strength 785 MPa), the safety factor is 1.8, exceeding the industry standard by 1.50, and it is 1.11 % higher than the original model. The maximum displacement in the *x* direction is 0.325 mm, and the stiffness is 1.67 °/m (with an increase of 0.60 %). The stiffness index needs to be optimized with emphasis. The minimum fatigue life is 321,380 times, exceeding the industry standard by 114 % and increasing by 8.18 % compared with the original model. The volume decreased from 670 cm^3 to 635 cm^3. The density was 7.87 g/cm^3, and the mass decreased from 5247 g to 4988 g (weight reduction of 4.31 % / 225.22 g).Detailed parameters are shown in the table below.

Table II: Comparison of flange fork parameters and performance.

Content	**Safety factor**	**Severity** /°/m	**Fatigue life / One million time**	**Quality** /g
Original parameters	1.80	1.66	297070	5226.29
After improvement	1.82	1.67	321380	5001.07
Rangeability	1.11 %	0.60 %	8.18 %	4.31 %
Industry requirement	1.50	15	150000	—

• **Improvement and analysis of universal joint fork**

The improved universal joint fork model was analysed by using the finite element analysis method and Settings consistent with the aforementioned, including the stress cloud map (Fig. 11 a), the Y-direction displacement cloud map (Fig. 11 b), and the fatigue life cloud map (Fig. 11 c).

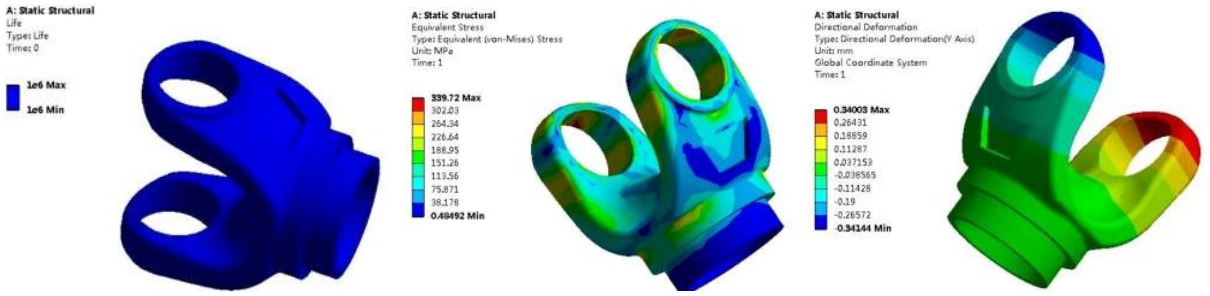

a) b) c)

Figure 11: The finite element analysis results of the improved universal joint fork model.

According to the data in Fig. 11, the maximum stress of the improved universal joint fork model is 339.72 MPa, the material yield strength is 785 MPa, the safety factor is approximately 2.31, which exceeds the industry standard by 1.50 and is 0.87 % higher than the original model. The stress safety margin is high. The maximum displacement in the Y direction is 0.34144 mm. According to the calculated stiffness, it is 1.53 °/m, with an increase of 1.32 %, demonstrating the structure's anti-deformation ability. The minimum fatigue life is 1 million times, far exceeding the industry's 150000 times and remaining on par with the original model. The weight was reduced by 713.89 g (a decrease of 11.47 %), achieving cost reduction and efficiency improvement as well as optimizing the overall vehicle performance. Table III clearly compares the performance parameters and quality differences between the original model and the improved model.

Table III: Comparison of universal joint parameters and performance.

Content	**Safety factor**	**Severity** /°/m	**Fatigue life / One million time**	**Quality** /g
Original parameters	2.29	1.51	100	6225.64
After improvement	2.31	1.53	100	5511.75
Rangeability	0.87 %	1.32 %	0.00 %	11.47 %
Industry requirement	1.50	15	15	—

5. CONCLUSION

Lightweight design strategies for the drive shaft components of light vehicles were investigated. Through finite element analysis and topology optimization techniques, improvements in structural performance and weight reduction were achieved. Specifically:

(1) Finite element static analysis was conducted on the flange of the drive shaft and the universal joint fork. The results indicated that key components possess lightweight potential while maintaining safety factors and durability, thus providing a foundation for subsequent topological optimization and contributing to enhanced fuel efficiency and vehicle performance.

(2) During the topology optimization phase, the SIMP variable density method was employed for optimizing the core shaft component with the objective of minimizing volume. The outcomes demonstrated significant weight reduction without compromising performance. However, due to the complex geometry of the optimized structure, further refinements are required to balance manufacturability and performance.

(3) Finally, based on improved designs of the flange and universal joint fork, finite element analysis validated the enhanced model in terms of safety coefficients, stiffness, and fatigue life. Key performance indicators showed notable improvements, such as a 4.31 % and 11.47 % reduction in mass, respectively. These achievements not only comply with industry standards but also offer valuable references for future lightweight design initiatives. Of course, the existing research mainly remains at the theoretical research stage and has certain limitations. The relevant simulation results can also be further verified physically, and then the transmission shaft components can be further lightweight by using high-performance materials.

REFERENCES

[1] Zhou, D.; Wang, Y.; Li, S.; Mao, X.; Zhou, C.; Kang, Z.; Su, X. (2025). Optimization of aluminum alloy steering knuckle for automotive lightweighting and performance enhancement, *Journal of the Brazilian Society of Mechanical Sciences and Engineering*, Vol. 47, No. 7, Paper 327, 20 pages, doi:10.1007/s40430-025-05575-0

[2] Lian, F.; Wang, D.; Zhang, Z.; Chen, H.; Xu, W. (2025). Multi-objective optimization of lightweight and crashworthiness of automotive front-end structures based on stacked regression surrogate, *Engineering Applications of Artificial Intelligence*, Vol. 155, Paper 111138, 16 pages, doi:10.1016/j.engappai.2025.111138

[3] Tarbajovsky, P.; Puskar, M.; Sabadka, D. (2023). Simulation model of vehicle emission reduction exhaust system, *International Journal of Simulation Modelling*, Vol. 22, No. 4, 679-689, doi:10.2507/IJSIMM22-4-675

[4] Liu, J. (2025). Optimization of efficiency maximization strategy of automobile transmission system based on simulated annealing algorithm, *Engineering Research Express*, Vol. 7, No. 1, Paper 015137, 15 pages, doi:10.1088/2631-8695/adc224

[5] Shen, Y.; Huang, J. (2025). Residual life forecasting and advanced surface damage remanufacturing processes for automotive drive axle shells, *Advances in Mechanical Engineering*, Vol. 17, No. 2, 17 pages, doi:10.1177/16878132251321054

[6] Reddy, P. S. K.; Nagaraju, C. (2017). Weight optimization and finite element analysis of composite automotive drive shaft for maximum stiffness, *Materials Today: Proceedings*, Vol. 4, No. 2, Part A, 2390-2396, doi:10.1016/j.matpr.2017.02.088

[7] Zhang, H.; Li, S.; Wu, Y.; Zhi, P.; Wang, W.; Wang, Z. (2024). A multiscale reliability-based design optimization method for carbon-fiber-reinforced composite drive shafts, *Computer Modeling in Engineering & Sciences*, Vol. 140, No. 2, 1975-1996, doi:10.32604/cmes.2024.050185

[8] Samuel, M.; Tayong, R. B. (2023). 3D numerical analysis of the structural behaviour of a carbon fibre reinforced polymer drive shaft, *Results in Engineering*, Vol. 18, Paper 101120, 7 pages, doi:10.1016/j.rineng.2023.101120

[9] Choi, J.-W.; Han, S.-H.; Lee, K.-H. (2021). Structural analysis and optimization of an automotive propeller shaft, *Advances in Mechanical Engineering*, Vol. 13, No. 10, 11 pages, doi:10.1177/16878140211053173

[10] Tian, Y. L.; He, J. L.; Niu, H. L. (2011). Self-development design of automotive transmission based on MASTA platform, *Advanced Materials Research*, Vols. 308-310, 2201-2204, doi:10.4028/www.scientific.net/AMR.308-310.2201

[11] Harl, B.; Predan, J.; Gubeljak, N.; Kegl, M. (2017). On configuration-based optimal design of load-carrying lightweight parts, *International Journal of Simulation Modelling*, Vol. 16, No. 2, 219-228, doi:10.2507/IJSIMM16(2)3.369

[12] Kim, T. A.; Park, H. J.; Han, S. H. (2019). Shape optimization design of an automotive drive shaft for improving fatigue life, *Transactions of the Korean Society of Mechanical Engineers A*, Vol. 43, No. 1, 67-72, doi:10.3795/KSME-A.2019.43.1.067

[13] Donmez, A.; Kahraman, A. (2025). An investigation of dynamic behavior of electric vehicle gear trains, *Journal of Computational and Nonlinear Dynamics*, Vol. 20, No. 2, Paper 021003, 16 pages, doi:10.1115/1.4067153

[14] Chen, Z.; Ju, Y.; Jia, Y.; Tang, W.; Wang, Y.; Li, S. (2024). Torsional vibration analysis and active anti-disturbance decoupling control of duplex trident universal joints, *Journal of Mechanical Science and Technology*, Vol. 38, No. 4, 1693-1702, doi:10.1007/s12206-024-0306-7

[15] Zhou, Q. H.; Zhu, X. Y.; Sun, J. M.; Li, J. (2022). Control of welding residual stress and deformation for the rod support of a crane, *International Journal of Simulation Modelling*, Vol. 21, No. 3, 501-512, doi:10.2507/IJSIMM21-3-CO12

[16] Harl, B. (2025). Effect of topological optimisation on the kinetic properties of the kinematic chain, *International Journal of Simulation Modelling*, Vol. 24, No. 1, 5-16, doi:10.2507/IJSIMM24-1-704

[17] Cui, X. Y.; Li, Z. Z.; Yin, B. L.; Wang, W. Q.; Liu, Y. X.; Bai, Z. H. (2023). Modelling analysis of coupling deformation between strip steel and roller system, *International Journal of Simulation Modelling*, Vol. 22, No. 2, 267-278, doi:10.2507/IJSIMM22-2-644

[18] He, D. X. (2024). Fault prediction in high-efficiency petroleum machinery production, *International Journal of Simulation Modelling*, Vol. 23, No. 1, 184-195, doi:10.2507/IJSIMM23-1-CO5

[19] Teli, S.; Surange, V.; Gaikwad, L. (2024). Failure analysis of automotive drive system: a Six Sigma DMADV approach, *Journal of Failure Analysis and Prevention*, Vol. 24, No. 5, 2292-2315, doi:10.1007/s11668-024-02003-8